

# Evaluation of Late Paleozoic Over-High Maturity Source Rocks in the Erlian Basin and Its Adjacent Areas

Tiantian Du<sup>a, \*</sup>, Yanxia Wang<sup>a</sup>, Yue Qu<sup>a, \*\*</sup>, Xuanlong Shan<sup>b</sup>, and Yuhang Shang<sup>a</sup>

<sup>a</sup> College of Mining Engineering, Heilongjiang University of Science and Technology, Heilongjiang, Harbin, 150022 PR China

<sup>b</sup> College of Earth Sciences, Jilin University, Jilin, Changchun 130061 PR China

\*e-mail: dutianzeus@126.com

\*\*e-mail: quyue@usth.edu.cn

Received March 2, 2023; revised April 22, 2023; accepted June 19, 2023

**Abstract**—The evaluation of Paleozoic source rocks during oil and gas exploration is important yet difficult. This study qualitatively and quantitatively evaluated the potential of Late Paleozoic source rocks through organic geochemical analyses of 18 outcrop samples from the Linxi, Zhesi and Benbatu formations in the Erlian Basin and its adjacent areas. The results revealed that Late Paleozoic source rocks are currently in a stage of over-high maturity. The three source rock intervals recorded low organic carbon contents (TOC) and low hydrocarbon generation potential. The abundance of organic matter (OM) was corrected to account for the effects of weathering and to calculate the original carbon content. The original hydrocarbon generation potential was determined using a chemical kinetics method. The average original TOC contents (TOC<sub>0</sub>) of the Linxi, Zhesi and Benbatu formations were 0.89, 0.28 and 0.17%, respectively, with average original hydrocarbon generation potentials (S<sub>20</sub>) of 2.171, 0.939 and 0.409 mg/g, respectively. The original abundance of OM met the standard of an effective source rock, and the mudstone of the Linxi Formation reached the standard of an effective source rock. The results of saturated hydrocarbon gas chromatography (GC) analysis using the Late Paleozoic source rocks in the Erlian Basin and its adjacent areas revealed obvious “bimodal” characteristics, and the main carbon peaks were distributed near C<sub>17–19</sub> and C<sub>23–25</sub>. These results suggested that the sources of OM were mainly low-level aquatic organisms, which are able to generate oil and gas. The obvious differences between the residual and original hydrocarbon generation potentials indicated that the Late Paleozoic source rocks generated and discharged hydrocarbons. Notably, the original hydrocarbon generation potential of the Linxi Formation mudstone is high.

**Keywords:** source rock, Late Paleozoic, Erlian Basin, over-high maturity, organic geochemistry

**DOI:** 10.1134/S0016702923110022

## INTRODUCTION

Source rock evaluation provides support for oil and gas exploration. In recent years, many articles about Mesozoic hydrocarbon source rock evaluation in the Erlian Basin have been published, but few studies have focused on Paleozoic source rock evaluation in the Erlian Basin. Paleozoic source rocks in the Erlian Basin have many characteristics that make them difficult to study, including their wide distribution, large thicknesses, deep burial depths, lack of previous drilling records, and severe surface weathering (Wang et al., 2008; Zhang et al., 2008; Han et al., 2011).

The abundance, type and maturity of organic matter (OM) are three main characteristics of Paleozoic source rock evaluation. Based on the determination of the total organic carbon (TOC) content and biomarker compound analysis, some scholars have determined that Devonian source rocks in western Canada contain a large amount of hydrocarbons. The TOC content of the Devonian source rocks reached up to

15%, and the depositional environment was an open marine to lagoonal setting (Fowler and Stasiuk, 2001). In the New Siberian Islands, where large quantities of dark mudstone were deposited during the Lower Devonian, the determination of the TOC content and Rock-Eval results demonstrated that the OM abundance in mudstone could reach the high-quality source rock standard (Sobolev et al., 2016). Based on the OM abundance results and associated optical characteristics, Silurian and Ordovician low-maturity shales were determined to represent the most productive hydrocarbon source rocks of kerogen in the Holy Cross Mountains of Poland (Schito et al., 2017). The results of Rock-Eval experiments and pollen analyses of Silurian source rocks in the Arabian Peninsula demonstrated that Lower Silurian shale is the best Paleozoic source rock in this region (Saber et al., 2016). Paleozoic source rock evaluations have also been conducted in the Tarim Basin, Sichuan Basin and Ordos Basin. In the Tarim Basin, the Lower Cam-

brian, Ordovician and Lower Ordovician dolomite strata are the main Paleozoic source rocks and have high OM contents (Zhao et al., 2008). In the Sichuan Basin, the Lower Cambrian Qiongzhusi Formation and the Lower Silurian Longmaxi Formation developed two sets of regional high-quality source rocks and formed multiple sets of source-reservoir-cap assemblages. Study results have indicated the favourable potential for petroleum exploration in the Sichuan Basin (Rao et al., 2013). The Ordovician-Permian source rocks in the Ordos Basin were also determined to have considerable gas generation potential (Liu et al., 2016). Paleozoic source rocks in the Erlian Basin were identified using organic geochemical methods (Han et al., 2011). These results indicated that the dark mudstone and carbonate layers contained enormous hydrocarbon generation potential. Based on a detailed research, Lower Silurian shale has recently been selected as an organic-rich shale layer (Chen et al., 2017b). A detailed exploration was conducted in NE China, and 188 Late Paleozoic samples were collected (Zhang et al., 2008). U-Pb dating, Rb-Sr dating and illite crystallization experiment results were used to analyse the tectonic and sedimentation characteristics. They determined that the dark mudstone strata in the Middle Permian marine sediments and the Late Permian continental sediments were high-quality source rocks. Source rock evaluation in the Erlian Basin has mostly been performed based on TOC evaluation, with less attention paid to the evaluation of the original hydrocarbon generation potential. Moreover, most studies have been based on analyses of outcrops, often ignoring the influences of weathering and the hydrocarbon generation on the OM abundance. Based on an analysis of Late Paleozoic outcrops in this study, a weathering correction is proposed in addition to a correction for the calculated original OM abundance. Specifically, TOC and  $S_2$  are corrected. When combined with OM source data, these results are used to determine the original hydrocarbon generation potential.

## GEOLOGICAL SETTINGS OF STUDY AREA

The Erlian Basin and its adjacent areas are located in the middle of the Inner Mongolia Autonomous Region, China. Tectonically, this area is located between the North China Plate and the Siberian Plate—an area that is also referred to as the Northeast Plate or the Jia-Meng Plate (Wang et al., 2008). The Xar Moron River fault zone represents the southern margin of this study area, which extends to the Greater Khingan Mountains along the Heganshan suture zone to the northeast. At the end of the Early Carboniferous, multiple palaeogeographic systems were combined together in the eastern region of Northeast China. The western region was still covered by seawater but experienced a decrease in sea level. Multiple sets of marine carbonate sediments were developed

from the Devonian to the Early Carboniferous. Complex tectonic movement occurred in this area at the beginning of the Early Permian, which was followed by multiple sealevel rise events. This caused both marine and continental sediments to exist simultaneously. At the end of the Permian, the ocean disappeared and formed the ancient Permian Basin (Zhang et al., 2008). The Erlian Basin is a Mesozoic continental basin that overlies the Late Paleozoic basement and has immense petroleum resource potential (Zhang et al., 2012; Zhai et al., 2015). The known source rock layers are all Mesozoic strata, which have generally developed in the mudstone strata of the Cretaceous Alshan Formation and Tengger Formation. Late Paleozoic strata have always been considered the basement of the Erlian Basin due to their wide distribution and large thicknesses (Fig. 1).

The lithology of the Carboniferous Benbatu Formation is mainly limestone with rich marine fossils. Additionally, the basin contains some clastic rocks and exhibits low-grade metamorphism. The Benbatu Formation is overlain by the Amushan Formation, and its exact bottom contact has not been found (Wang et al., 2008). Clastic rocks and bioclastic limestone are the main lithologies in the Permian Zhesi Formation. The Zhesi Formation is overlain by the Linxi Formation and bordered to the bottom by the Dashizhai Formation. The Zhesi Formation is widely exposed in the Erlian Basin and the surrounding areas, including the Suolun region and the West Ujimqin banner region in Inner Mongolia. The formation can reach a thickness of thousands of metres. A large number of microorganism fossils have been found in the Zhesi Formation (Zhai et al., 2015). In addition, analyses of its sedimentary facies have revealed that the lower layers of the Zhesi Formation are composed of neritic facies (Zhang et al., 2008).

The Linxi Formation comprises a sequence of sedimentary rocks that is thousands of metres thick. Influenced by Variscan movement, the Erlian Basin and its adjacent areas experienced a “littoral-bathyal-delta front-bathyal-littoral” evolution. By the end of the Late Permian, the land had completely formed (Zhai et al., 2015). In this region, Carboniferous and Permian outcrops with obvious weathering effects are widely distributed. Additionally, relatively few wells have been drilled into Paleozoic strata (Fig. 1). All these factors increase the difficulty of performing evaluations of Paleozoic hydrocarbon source rock.

## EXPERIMENTAL MATERIALS AND METHODS

### *Experimental Materials*

Eighteen Paleozoic samples were collected in the study area for TOC, Rock-Eval, soluble OM, kerogen and saturated hydrocarbon GC analyses. The samples were obtained from three measured sections of lime-

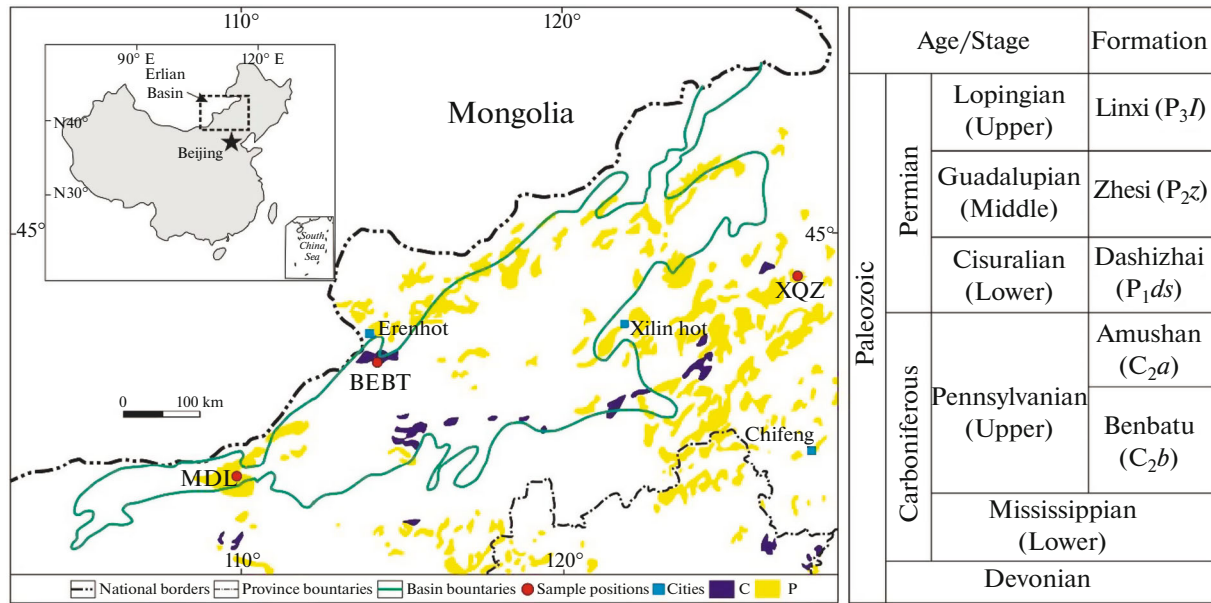


**Fig. 1.** Location of the study area, distributions of Late Paleozoic outcrops and sample positions, and Late Paleozoic stratigraphy (based on Liu et al., 2011).

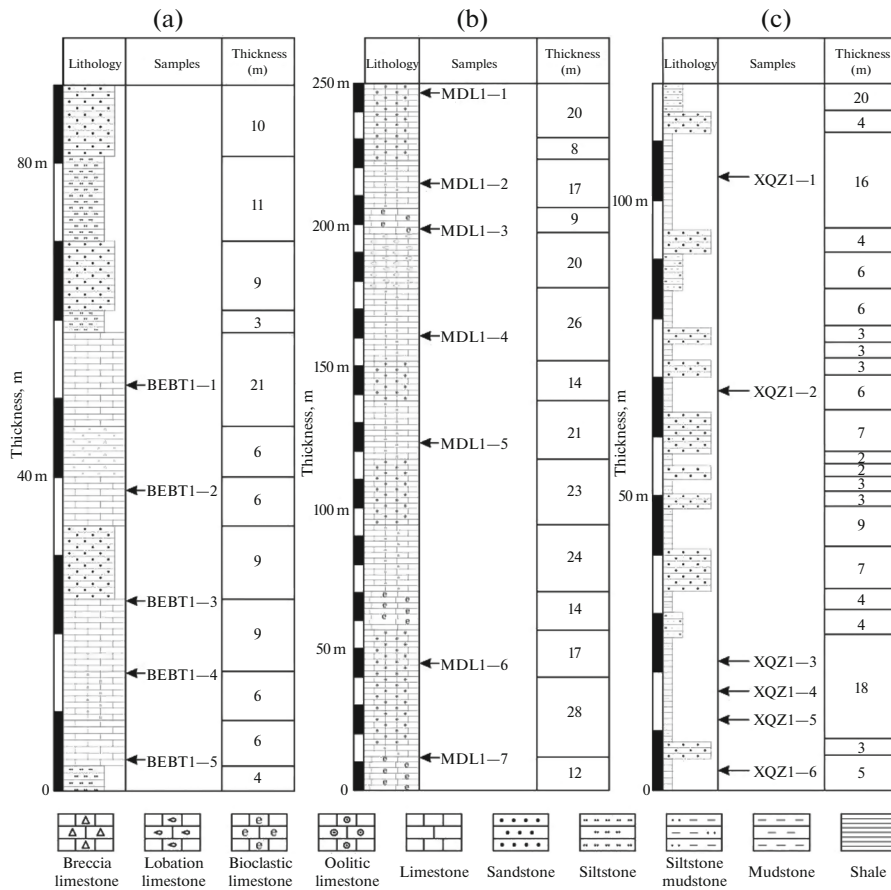


**Fig. 2.** Field sections and sample positions. (a) Carboniferous measured section from the Benbatu Formation in the Baobenbatu area. (b) Permian measured section from the Zhesi Formation in Mandula Town. (c) Permian measured section from the Linxi Formation in Linxi County.

stone and mudstone layers in the field (Fig. 2). Five limestone and breccia limestone samples (from BEBT1-1 to BEBT1-5) were collected from the Carboniferous Benbatu Formation in the Baoenbatu area (Fig. 2a). Additionally, seven samples (from MDL1-1 to MDL1-7) were collected from the Permian Zhesi Formation in Mandula Town, and these samples contain oolitic limestone, breccia limestone and bioclastic limestone (Fig. 2b). Finally, six mudstone samples (from XQZ1-1 to XQZ1-6) were collected from the Permian Linxi Formation in Linxi County (Fig. 2c).

### Experimental Methods

The OM abundance is mainly determined via TOC content, Rock-Eval, soluble OM content and compositional analyses. Organic kerogen macerals are identified and used to evaluate the type of OM and determine the vitrinite reflectance. Additionally, these results can be combined with the results of saturated GC to evaluate the OM maturity (Tissot and Welte, 1984; Zhang et al., 2012).

**TOC content.** The United States LECO company carbon and sulphur tester (LECO-CS844) was used to determine the TOC content. The samples were first immersed in hydrochloric acid to remove inorganic carbon from the rocks and were then combusted at high temperatures. After the samples were fully oxidized, the content of organic carbon was calculated based on its combustion products ( $\text{CO}_2$ ). The TOC content was the ratio of organic carbon mass to the sample mass.

**Rock-Eval Analysis.** Rock samples were analysed via Rock-Eval pyrolysis under inert gas conditions and heated in stages. The instrument used was a YQ-6 from the Chinese Haicheng Company. The hydrocarbons and  $\text{CO}_2$  contents from the OM in the rocks were quantitatively analysed using a flame ionization detector and a thermal conductivity detector, respectively (Espitalie et al., 1985). The pyrolysis parameters used in this research included  $S_1$  (the hydrocarbon content per unit mass of rock under  $300^\circ\text{C}$ ) and  $S_2$  (the hydrocarbon content per unit mass of rock from  $300$  to  $600^\circ\text{C}$ ). The hydrocarbon generation potential was calculated by summing  $S_1$  and  $S_2$ . In this study, the values of  $S_1$  were extremely small and only one-tenth of the values of  $S_2$  due to their high maturity. Therefore, the hydrocarbon generation potential was determined using the parameter  $S_2$ .

**Soluble OM extraction and compositional analysis.** Soluble OM is typically determined using the Soxhlet extraction method. Samples were placed in an extractor after being crushed. Then, the soluble OM from the samples was dissolved continuously using an organic solvent, such as chloroform, under heating conditions. The content of extracted OM was called chloroform bitumen "A", which represents the content of soluble OM in these rocks.

The hydrocarbon forms of chloroform bitumen "A" included saturated hydrocarbons, aromatic hydrocar-

bons, non-hydrocarbons and asphaltene. Asphaltene was precipitated using *n*-hexane. Then, the samples were placed in a mixture column to undergo separation. Petroleum ether, benzene and an ethanol-benzene mixed solution were used to elute saturated hydrocarbons, aromatic hydrocarbons and non-hydrocarbons, respectively. The content of each component was then determined. The total hydrocarbon content was the sum of the saturated hydrocarbons and aromatic hydrocarbons.

**Identification of organic kerogen macerals and determination of vitrinite reflectance.** Kerogen must be separated from rock samples prior to identification. A biological microscope (Zeiss Axioskop 2 Plus, Germany) was used to identify and quantify different types of organic macerals. There are four types of organic macerals, and all have different characteristics. These macerals can be differentiated under the microscope based on several characteristics (Teichmüller and Wolf, 1977; Clayton, 1978). Carbonates and silicate minerals were first removed from each sample via a repeated hydrochloric acid and hydrofluoric acid treatment; then, chloroform was used to remove soluble OM. After heavy minerals were removed using the heavy liquid flotation method, the remaining residual matter was kerogen. Various components were identified by transmission and fluorescence microscopy, and different types of kerogen were classified using the Type Index (TI). TI values were determined based on experiments involving kerogen macerals but can be calculated for different types of "organic macerals". The TI formula is as follows:

$$TI = 100a + 80b_1 + 50b_2 + (-75)c + (-100)d,$$

TI—Type Index;

*a*—the content of sapropelic groups, %;

*b*<sub>1</sub>—the content of resinite, %;

*b*<sub>2</sub>—the total content of sporinite and cutinite, %;

*c*—the content of vitrinite, %;

*d*—the content of inertinite, %.

The classification standard of OM types is as follows:

*TI* > 80, sapropelic kerogen, type I;

*TI* from 40 to 80, sapropelic-humic kerogen, type II<sub>1</sub>;

*TI* from 0 to 40, humic-sapropelic kerogen, type II<sub>2</sub>; and

*TI* < 0, humic kerogen, type III (Hou, 2011).

After drying for 12 h, highly polished rock samples were observed under reflected light using a microscope (MPV type, 20×) from the Leitz Company, Germany. The reflected light signal emitted from the microscope was projected onto the sample surface. Then, a Deta V4000-SP Type spectrophotometer from the Y-3 Company, United States, was used to receive the beam reflected from the samples. In the spectrophotometer, different wavelengths of the beam were separated and converted to electrical signals. The

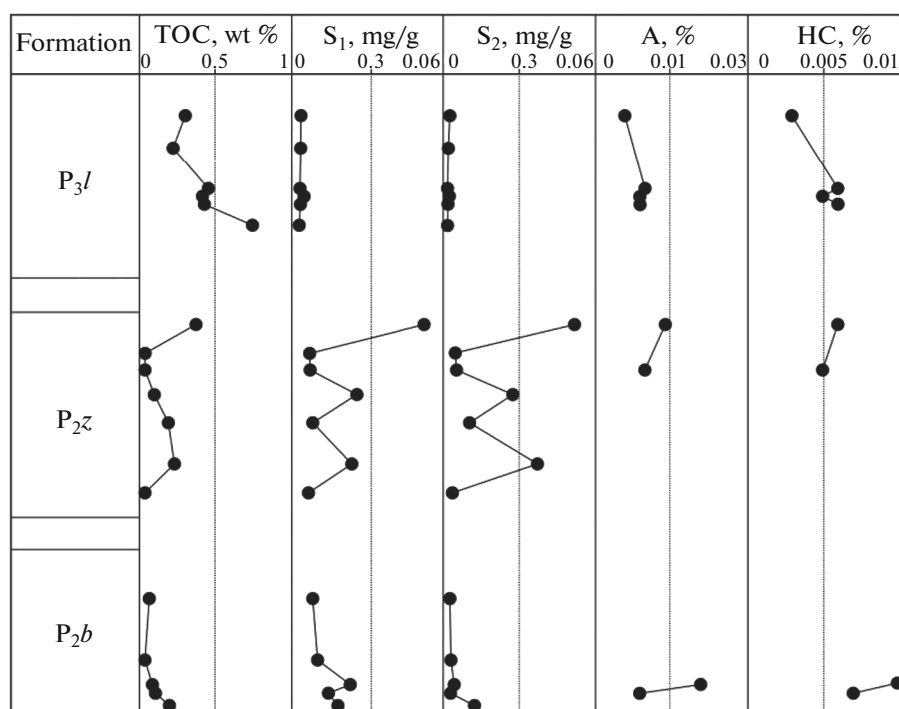


Fig. 3. Results of measured organic matter abundance.

reflected light intensity of the vitrinite from the samples was calculated by counting these electrical signals. Vitrinite reflectance (R<sub>o</sub>) was calculated as the percentage of the reflected light intensity from the polished vitrinite surface relative to the intensity of the incident light (from the master standard) at a wavelength of 549 nm. At least 30 points were measured on each sample, and the maximum value was used (Bertrand, 1990; Hou, 2011).

**Saturated hydrocarbon GC analysis.** A gas chromatograph (Type HP-5890 from Agilent Company, United States) was used in this study for saturated hydrocarbon GC. The extracted saturated hydrocarbon samples were placed into a gas chromatograph and separated in the capillary column using nitrogen gas. The carrier gas rate was 20 cm/s. A fused silica capillary column (FSOT) was used in the analysis, and the stationary phase was methyl silicone. The injector temperature was 310°C, and the temperature of the inspection room was 320°C. The start temperature of the column was 40°C, which was maintained for 10 min. Then, the temperature was increased at a rate of 3°C/min to 310°C, and this temperature was held until no peaks appeared. The resulting product was analysed with a flame ionization detector to determine its components.

## RESULTS AND DISCUSSION

### Results

Table 1 and Fig. 3 present the results of the TOC measurements and Rock-Eval pyrolysis. The TOC

Table 1. TOC and Rock-Eval pyrolysis results

Sample	TOC, wt %	S <sub>1</sub> , mg/g	S <sub>2</sub> , mg/g	T <sub>max</sub> , °C	"A", %	HC, %
XQZ1-1	0.30	0.004	0.026	315	0.006	0.003
XQZ1-2	0.22	0.004	0.017	525	—	—
XQZ1-3	0.45	0.003	0.010	316	0.010	0.006
XQZ1-4	0.42	0.005	0.022	413	0.009	0.005
XQZ1-5	0.43	0.003	0.010	315	0.009	0.006
XQZ1-6	0.74	0.003	0.015	525	—	—
MDL1-1	0.37	0.052	0.518	436	0.014	0.006
MDL1-2	0.02	0.007	0.047	497	—	—
MDL1-3	0.03	0.007	0.053	509	0.010	0.005
MDL1-4	0.10	0.026	0.274	435	—	—
MDL1-5	0.19	0.008	0.104	439	—	—
MDL1-6	0.23	0.024	0.371	433	—	—
MDL1-7	0.03	0.007	0.037	499	—	—
BEBT1-1	0.07	0.008	0.026	495	—	—
BEBT1-2	0.03	0.010	0.031	479	—	—
BEBT1-3	0.08	0.023	0.045	438	0.021	0.011
BEBT1-4	0.11	0.014	0.029	475	0.009	0.007
BEBT1-5	0.20	0.018	0.123	438	—	—

TOC—Total organic carbon content, wt %.

S<sub>1</sub>—Hydrocarbon content per unit mass of rock under 300 °C, representing the free hydrocarbon content, mg/g.

S<sub>2</sub>—Hydrocarbon content per unit mass of rock between 300 °C and 600 °C, representing the hydrocarbon generation potential, mg/g.

"A"—Chloroform bitumen "A" content, %.

HC—Total hydrocarbon content, %

**Table 2.** Kerogen microstructure results

Sample	Sapropelic, %	Exinite, %	Vitrinite, %	Inertinite, %	<i>TI</i>	Type
BEBT1-5	20	2	30	48	−49.5	III
MDL1-1	35	2	30	33	−19.5	III
MDL1-5	15	1	30	54	−61	III
MDL1-6	15	—	45	40	−58.75	III
XQZ1-1	71	—	—	29	42	II <sub>1</sub>
XQZ1-2	72	—	—	28	44	II <sub>1</sub>
XQZ1-3	71	—	—	29	42	II <sub>1</sub>
XQZ1-4	82	—	—	18	64	II <sub>1</sub>
XQZ1-5	85	—	—	15	70	II <sub>1</sub>
XQZ1-6	75	—	—	25	50	II <sub>1</sub>

*TI*—Type Index; Type—Kerogen type of OM

contents of most samples are below 0.5 wt%, and  $S_2$  is generally below 0.5 mg/g.

**Linxi Formation.** The average TOC content of the Linxi Formation samples is 0.43%, although TOC values range from 0.22 to 0.74%. The  $S_2$  values range from 0.01 to 0.026 mg/g, with an average value of 0.017 mg/g. The values of chloroform bitumen “A” from four Linxi Formation samples range between 0.006 and 0.01% (Table 1; Fig. 3). The OM type is type II<sub>1</sub> based on the *TI* index, the values of which range from 42 to 70. The values of  $R_o$  are greater than 1.2%, with a maximum of 2.18% (Table 1). Additionally, the  $R_o$  results indicate that the Linxi Formation mudstone is a high-maturity source rock (Bertrand, 1990).

**Zhesi Formation.** The measured TOC values of the Zhesi Formation range from 0.02 to 0.37 wt%, with an average value of 0.14%. The values of  $S_2$  range from 0.037 to 0.518 mg/g, with an average value of 0.201 mg/g. The values of chloroform bitumen “A” from two samples are 0.014 and 0.01% (Table 1; Fig. 3).

**Table 3.** OM maturity results

Formation	Sample	Lithology	$R_o$ , %	OEP
$C_2b$	BEBT1-3	Limestone	—	0.93
$C_2b$	BEBT1-5	Limestone	—	0.98
$P_2z$	MDL1-1	Limestone	—	1.01
$P_2z$	MDL1-3	Limestone	—	0.9
$P_3l$	XQZ1-1	Mudstone	1.30	—
$P_3l$	XQZ1-2	Mudstone	1.48	—
$P_3l$	XQZ1-3	Mudstone	2.03	1.04
$P_3l$	XQZ1-4	Mudstone	1.54	1.02
$P_3l$	XQZ1-5	Sandstone	2.04	0.96
$P_3l$	XQZ1-6	Sandstone	2.18	—

$R_o$ —Vitrinite reflectance; OEP—Odd-even predominance (Scalan and Smith, 1970)

Additionally, the total hydrocarbon contents of the samples are 0.006 and 0.005%. The *TI* values range from −60 to −19.5, and the main type of kerogen is type III based on the *TI* classification standard discussed above (Table 2). According to the OEP indexes, the OM reached the mature stage (Scalan and Smith, 1970).

**Benbatu Formation.** The measured TOC values of the Benbatu Formation range from 0.03 to 0.2 wt %, with an average value of 0.1 wt %. The calculated  $S_2$  values range from 0.026 to 0.123 mg/g, with an average of 0.051 mg/g. The chloroform bitumen “A” values of the Benbatu Formation are 0.021 and 0.009% based on the results of only two samples. The total hydrocarbon contents of these two samples are 0.011 and 0.007% (Table 1; Fig. 3). The OM type is type III based on the *TI* classification standard discussed above (Table 2). In this study, available vitrinites were rarely found in limestone samples; thus, the OEP index was applied to determine the maturity of the limestone samples. The calculated OEP index values are approximately 1 (Table 3), indicating that their evolution reached the mature stage (Scalan and Smith, 1970).

The  $T_{max}$  values of the samples in this study were highly volatile. The values ranged from 315 to 525°C for eighteen samples. Even in the same section, the maximum and minimum  $T_{max}$  values exhibited differences of 100°C or more. Evaluating the OM maturity based on  $T_{max}$  can be influenced by the OM type, the values of  $S_1$  and the expulsion efficiency of hydrocarbon. Thus, due to the extremely low  $S_1$  values in this study, the volatile  $T_{max}$  values cannot be used to evaluate the OM maturity (Chen et al., 2017a).

### Discussion

**Determination of the original organic matter abundance.** The parameters of OM abundance are indexes can be used to evaluate source rocks. However, the measured abundance of OM represents the residual

**Table 4.** Weathering correction coefficients of organic carbon in different areas and this study

Study area	Age	Lithology	Climate	Coefficient	Data source
Kaili and Shiqian areas	S–O	Limestone	Subtropical monsoon	1.55–3.45	Li, 1985
Qinshui Basin	C	Limestone	Temperate continental	2.49	Zhang, 2001
Daijiagou area, Chongqing	T <sub>1</sub>	Limestone	Subtropical monsoon	1.25	
	P <sub>2</sub>	Mudstone		1.45	
Ejin Banner, Inner Mongolia	C–P	Mudstone	Temperate continental	1.08–1.67	Wei, 2012
Northern Tarim Basin	C	Limestone	Plateau continental	1.20	Yang, 2016
Erlian Basin and adja- cent areas	P <sub>3</sub> <i>l</i>	Mudstone	Temperate continental	1.67	This study
	P <sub>2</sub> <i>z</i>	Limestone		1.54	
	C <sub>2</sub> <i>b</i>	Limestone		1.45	

Coefficients—Weathering correction coefficients.

content remaining after hydrocarbon generation and expulsion. Therefore, the original OM abundance of highly mature source rocks must be determined. The OM content of rocks is reduced by the effects of hydrocarbon generation and expulsion (Cooles, 1986; Lu et al., 2003). Additionally, samples collected from outcrops have undergone weathering that differs from that experienced by underground samples and affects the indexes of OM abundance (Marynowski et al., 2011; Rao et al., 2013). Therefore, applying a weathering correction is necessary for determining the original OM abundance of Late Paleozoic highly mature source rocks. Because the parameters of chloroform bitumen “A” and total hydrocarbon are greatly affected by the complex process of weathering, these parameters were not assessed in this study.

**Weathering correction.** Due to the complexity of weathering and the uncertainty of the exposure time, it is difficult to infer the entire weathering process. TOC values were measured from outcrops and underground samples to calculate weathering correction coefficients (Colman, 1981; Li, 1985; Zhang et al., 2001; Wei et al., 2012; Yang et al., 2016). The Erlian Basin and its adjacent areas are characterized by a low degree of exploration and relatively little drilling. An analogous method was used to determine the TOC weathering correction coefficients in this study by comparing the age, sedimentary environment, OM maturity and climate factors of different samples (Table 4).

Highly mature Carboniferous-Permian mudstones were studied in the Ejin Banner, Inner Mongolia (Wei et al., 2012), they considered the maximum depth influenced by weathering to be 50 metres. Additionally, a series of weathering correction coefficients were obtained which ranged from 1.08 to 1.67. The magnitude of these coefficients increased from a depth of 50 m to the surface. The study area analysed here is located at the same latitude as the Ejin Banner area. The two areas also have the same surface climate, which is a temperate continental climate. Because the

mudstone samples in this study were collected from the surface, their weathering correction coefficient was determined to be 1.67 based on the maximum value obtained by Wei et al., (2012). The weathering factors of Paleozoic source rocks were previously studied by Zhang et al., (2001), whose results revealed that the anti-weathering ability of rock decreases with increasing shale content. Therefore, the anti-weathering ability of limestone is stronger than that of mudstone; thus, it has a smaller weathering correction coefficient. Through comparing precipitation, climate and wind power factors in the Qinshui Basin, Tarim Basin and areas studied here, a maximum weathering correction coefficient of 2.49 was obtained in the Qinshui Basin, while a minimum value of 1.20 was obtained in the Tarim Basin (Wei et al., 2012; Yang et al., 2016). Therefore, the weathering correction coefficient of the limestone from this study should fall between 1.20 and 2.49. Furthermore, it is likely less than that of mudstone, which ranges from 1.20 to 1.67. Studies of ancient environments indicate that the environment was more stable when the Benbatu Formation was deposited. Therefore, the coefficient of the Benbatu Formation should be greater than that of the Zhesi Formation (Wang et al., 2008). The coefficients of these three formations were determined, as shown in Table 4.

S<sub>2</sub> is the measured hydrocarbon content per unit mass of rock at a temperature between 300 and 600°C, which represents the generated hydrocarbon content. The sum of S<sub>1</sub> and S<sub>2</sub> is generally used as a parameter for studying the hydrocarbon generation potential (Hatampour, 2014). However, due to the highly mature stages of these samples, the measured S<sub>1</sub> values were extremely small (Table 1) and contributed minimally to the sum of S<sub>1</sub> and S<sub>2</sub>. Therefore, only S<sub>2</sub> was corrected. By ignoring S<sub>1</sub>, the TOC loss actually represents the loss of the carbon content of S<sub>2</sub> after weathering (Espitalie et al., 1985). TOC and S<sub>2</sub> are relative



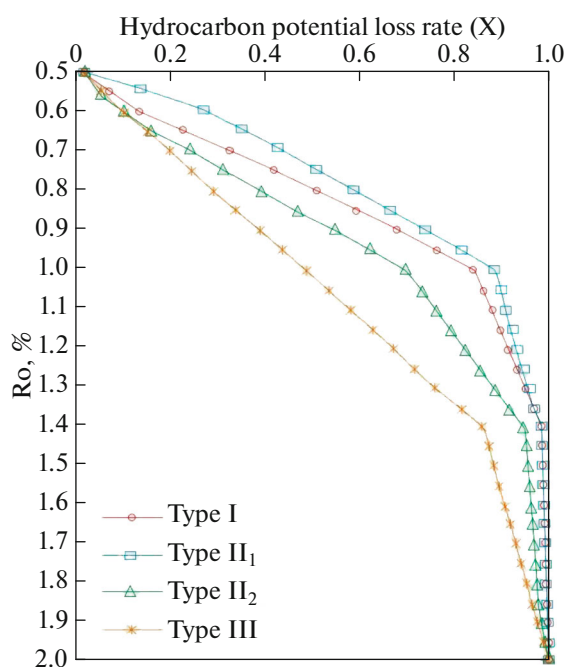


Fig. 4. The standard chart of the hydrocarbon potential loss rate (X) based on different OM types and maturity stages (Ro) (Lu et al., 2003).

Table 5. Results of TOC<sub>0</sub> and S<sub>20</sub>

Sample	TOC, wt %	S <sub>2</sub> , mg/g	TOC <sub>w</sub> , wt %	TOC <sub>0</sub> , wt %	S <sub>20</sub> , mg/g
XQZ1-1	0.30	0.026	0.501	0.58	0.961
XQZ1-2	0.22	0.017	0.3674	0.57	2.522
XQZ1-3	0.45	0.010	0.7515	0.89	1.643
XQZ1-4	0.42	0.022	0.7014	0.99	3.669
XQZ1-5	0.43	0.010	0.7181	0.85	1.710
XQZ1-6	0.74	0.015	1.2358	1.44	2.523
MDL1-1	0.37	0.518	0.5698	0.73	2.425
MDL1-2	0.02	0.047	0.0308	0.05	0.221
MDL1-3	0.03	0.053	0.0462	0.07	0.246
MDL1-4	0.10	0.274	0.154	0.23	1.284
MDL1-5	0.19	0.104	0.2926	0.33	0.488
MDL1-6	0.23	0.371	0.3542	0.47	1.738
MDL1-7	0.03	0.037	0.0462	0.06	0.174
BEBT1-1	0.07	0.026	0.1015	0.11	0.208
BEBT1-2	0.03	0.031	0.0435	0.06	0.247
BEBT1-3	0.09	0.045	0.1305	0.15	0.360
BEBT1-4	0.11	0.029	0.1595	0.17	0.237
BEBT1-5	0.20	0.123	0.29	0.36	0.992

TOC<sub>w</sub>—represents the content after applying the weathering correction (wt %).

TOC<sub>0</sub>—Original TOC content, which represents the content after applying the weathering correction and calculating the original abundance (wt %).

S<sub>20</sub>—Original hydrocarbon generation potential, which represents the content after applying the weathering correction and calculating the original abundance (mg/g).

values with the same denominator (rock mass); thus, the coefficient of S<sub>2</sub> is the same as that of TOC.

#### Determining the original organic matter abundance.

The absolute OM content in a rock decreases with increasing hydrocarbon generation and expulsion (Pepper, 1991; Esemé et al., 2007; Vandenbroucke and Largeau, 2007). Therefore, the determination of original OM abundance is necessary for source rock evaluation. Changes in hydrocarbon generation potential in the burial stage were simulated by using a chemical dynamics method (Lu et al., 2003). Lu (2003) established a standard chart defining the relationships between the loss rate of the OM generation potential, OM type and OM maturity (Fig. 4). The advantage of this method is that only the kerogen type and maturity are considered. The effects of the lithology, hydrocarbon expulsion efficiency and inorganic carbon on the recovery coefficient are excluded, making the approach suitable for the analysis of high-maturity source rocks. As noted above, the definition of hydrocarbon generation potential is (S<sub>1</sub> + S<sub>2</sub>), but S<sub>1</sub> can be ignored in this case. Therefore, the hydrocarbon generation potential in this study is actually the value of S<sub>2</sub>.

Figure 4 compares the hydrocarbon generation potential loss rates (defined as X) of different types of samples and samples of different maturity stages (Lu et al., 2003). As discussed above, the mature stages of the limestone samples from the Linxi Formation and the Benbatu Formation were determined by OEP. The OEP results indicate that the limestone samples from these two formations reached the mature stage, which suggests that Ro is greater than 1.2%. Since Ro spanned a range of values in the mature stage, the loss rate (X) applied corresponded to the smallest Ro value (Fig. 4). Therefore, the X of the limestone samples was determined for an Ro equal to 1.2% (Fig. 4). The loss rate (X) of the Zhesi Formation is 0.67, and that of the Benbatu Formation is 0.82 (Fig. 4; Table 5). The measured Ro values of the Linxi Formation samples are available and can be applied directly, but the Ro values of XQZ1-3, XQZ1-4 and XQZ1-5 are all greater than 2.0%. Therefore, the loss rate when Ro is equal to 2.0% (X) was applied (Fig. 4; Table 5).

The formula used to calculate the original hydrocarbon generation potential (S<sub>2</sub>) is as follows:

$$S_{20} = S_2 / (1 - X), \quad (1)$$

where S<sub>20</sub> is the original hydrocarbon generation potential and X is the hydrocarbon generation loss rate.

TOC<sub>0</sub> can also be calculated via the following formula:

$$TOC_0 = TOC + DTOC, \quad (2)$$

where TOC is the total TOC content measured from samples, which represents the residual content, and DTOC is the loss of organic carbon that occurs during the thermal evolution process.



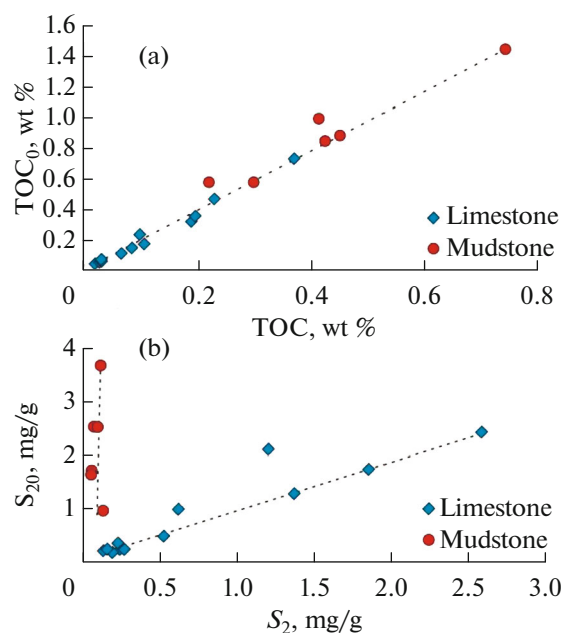


**Fig. 5.** Effects of restoring the original OM abundance between limestone and mudstone; (a) is the ratio between the original and measured TOC; and (b) is the hydrocarbon generation potential.

Based on the definition of TOC (Hou, 2011), formula (2) can be transformed into the following expression.

$$\text{TOC}_0 = \text{TOC} + 0.083(\text{S}_{20} - \text{S}_2). \quad (3)$$

The results obtained after performing the weathering correction and original abundance calculation are listed in Table 5.

The average value of  $\text{TOC}_0/\text{TOC}$  is 2.0, and the  $\text{S}_{20}/\text{S}_2$  results exhibit different characteristics that correspond to lithological differences (Fig. 5). The  $\text{S}_{20}/\text{S}_2$  values of the mudstone samples are greater than those of the limestone samples (Fig. 5). The  $\text{S}_{20}$  and  $\text{TOC}_0$  values of the samples from the Linxi Formation are higher than those of the Zhesi Formation and Benbatu Formation (Fig. 6). Over-high maturity mudstones lose more hydrocarbons during the processes of hydrocarbon generation and weathering. Based on the standards of source rock evaluation established by domestic and international scholars, the samples of the three formations in this study generally meet the effective source rock standard (Lu et al., 2003).

**Analysis of OM sources.** Low-level aquatic organisms contain low carbon number n-alkanes. By contrast, high-level plants are rich in waxes and mainly comprise high carbon number components (Didyk et al., 1978). The main carbon peaks of the Late Paleozoic samples all occur before  $\text{C}_{27}$  and exhibit an obvious “bimodal” characteristic, as they are mainly distributed near  $\text{C}_{17-19}$  and  $\text{C}_{23-25}$  (Fig. 7). These results reveal that the main sources of this OM are low-level aquatic organisms.

The contents of sapropelic groups and vitrinite in the Zhesi Formation samples are 35 and 30%, respectively (Table 2). Sapropelic groups are composed of

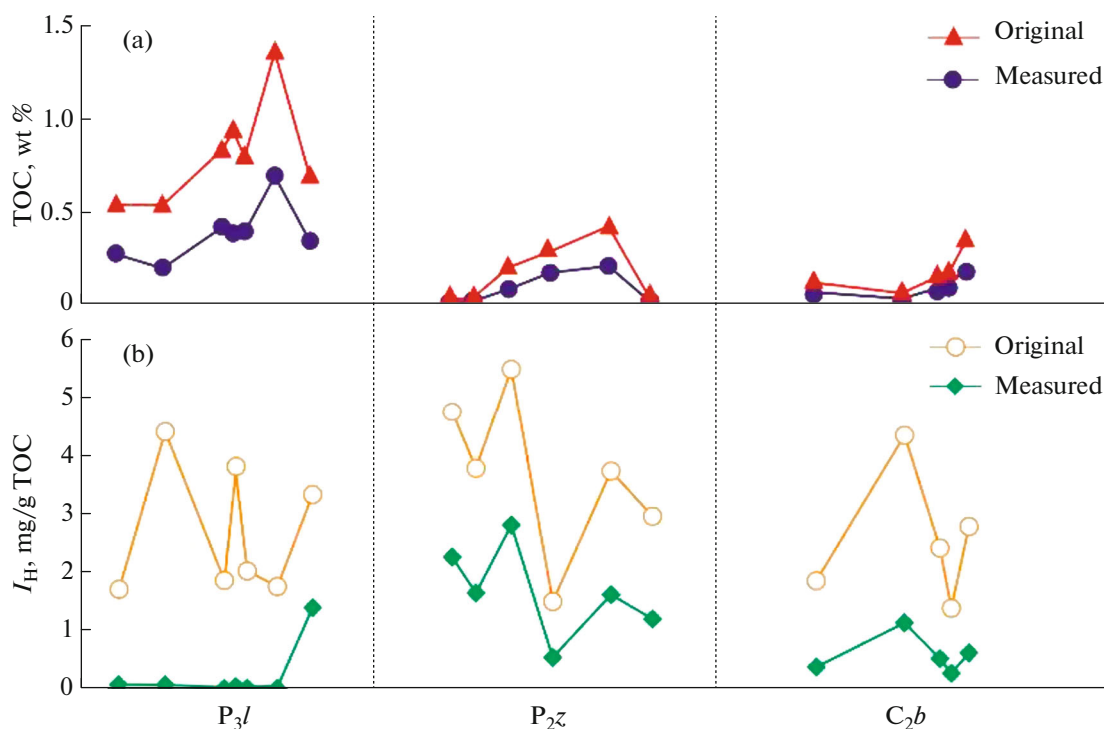


**Fig. 6.** Effects of restoring the original OM abundances of the Linxi Formation ( $\text{P}_3l$ ), Zhesi Formation ( $\text{P}_2z$ ) and Benbatu Formation ( $\text{C}_2b$ ); (a) is the ratio between the original and measured TOC; and (b) is the hydrocarbon generation potential.

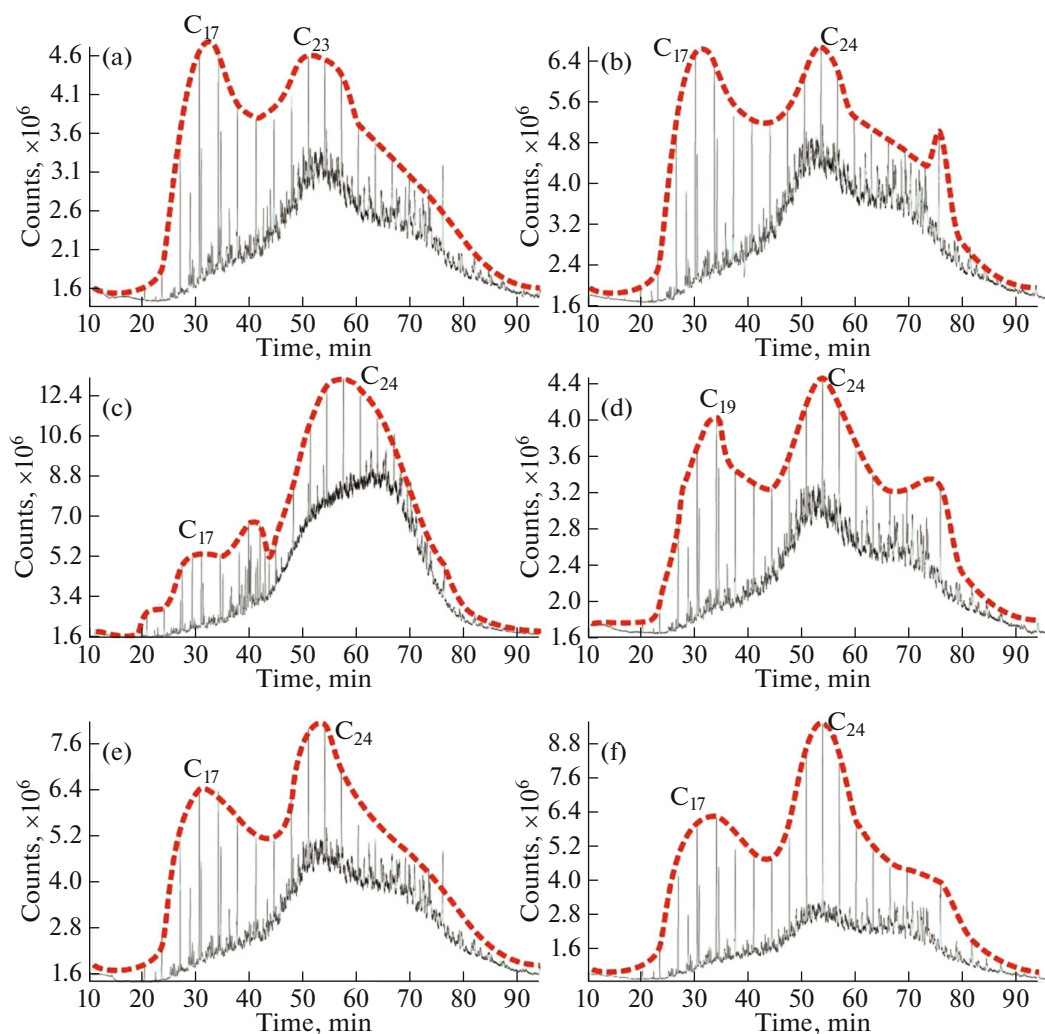


**Fig. 7.** Gas chromatographic characteristics of saturated hydrocarbons; (a) sample MDL1-1 from the Zhesi Formation; (b) sample MDL1-3 from the Zhesi Formation; (c) sample BEBT1-18 from the Benbatu Formation; (d) sample BEBT1-23 from the Benbatu Formation; (e) sample XQZ1-21 from the Linxi Formation; and (f) sample XQZ1-22 from the Linxi Formation.

flocculent and lump amorphous components (Fig. 8a). Bacteria and algae are the main sources of sapropelic groups with favourable hydrocarbon generation potential. Vitrinite groups are mostly tan tubes with weak fluorescence that are able to generate natural gas (Fig. 8b). The kerogen macerals in the Benbatu Formation are the same as those in the Zhesi Formation. However, the contents of the sapropelic groups are smaller at certain levels of fluorescence (Figs. 8c, 8d).

The identification results of organic kerogen macerals indicate that the kerogen type of the limestone of the Benbatu and Zhesi Formations is type III, mainly due to its high inertinite content (Table 2). This inertinite mainly originates from the wood fibre of high-level plants or the highly oxidized products of OM; however, the results of GC indicate that there are no high-level plant sources in these samples. During the Late Paleozoic, the marine facies environment gradually transformed to a land facies environment accom-

panied by the strengthening of oxidation. In this highly oxidized shallow sea sedimentary environment, residual low-level aquatic organisms formed inertinite groups, and the remaining unoxidized algae and bacterial residues formed sapropelic groups and other components (Scalan and Smith, 1970; Didyk et al., 1978).

The sapropelic contents of samples in the Linxi Formation are high, with some samples yielding values above 80% (Table 2). These components are non-transparent and display no fixed profile under transmitted light (Fig. 8e). Due to its high degree of thermal evolution, this stage of kerogen in the Linxi Formation samples represents the final phase of hydrocarbon generation. Because they have low residual hydrocarbon contents, these samples exhibit weak fluorescence (Fig. 8f).

The organic kerogen maceral identification and saturated hydrocarbon GC analysis results indicate

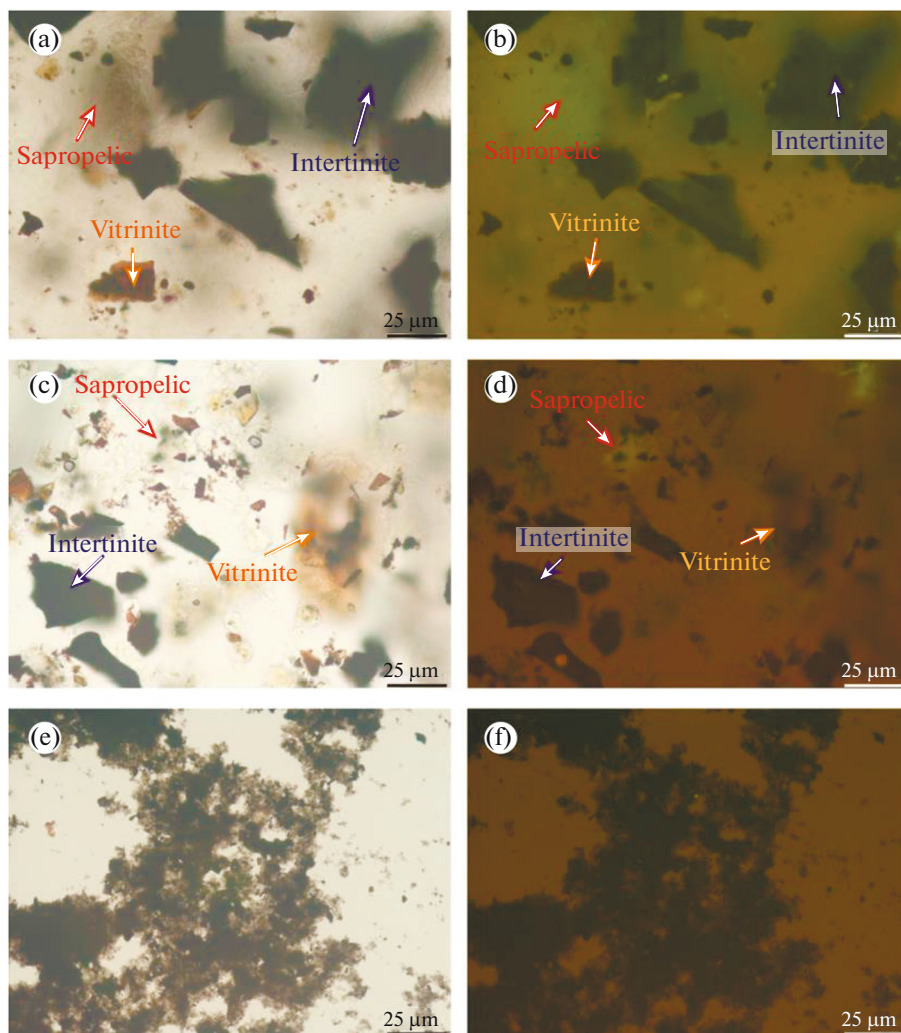


**Fig. 8.** Microphotographs of kerogen macerals in the studied source rocks from the Erlian Basin and its adjacent areas. (a) sample MDL1-1, Zhesi Formation, under transmitted light; (b) sample MDL1-1, Zhesi Formation, under fluorescent light; (c) sample BEBT1-25, Benbatu Formation, under transmitted light; (d) sample BEBT1-25, Benbatu Formation, under fluorescent light; (e) sample XQZ1-22, Zhesi Formation, under transmitted light; and (f) sample XQZ1-22, Zhesi Formation, under fluorescent light.

that the sources of kerogen are low-level aquatic organisms from the ocean and mainly include algae, bacteria and other zooplanktons. These residual organisms formed kerogen groups in source rock layers within transitional facies, which varied from marine to continental facies. These sources provided a material basis for the generation and expulsion of gas for the highly mature source rocks.

### CONCLUSIONS

Three Late Paleozoic source rock formations, which are very thick and widely distributed, have developed in the Erlian Basin and its adjacent areas. The results of organic geochemical analysis indicate that these three source rock formations have low residual OM abundance and poor residual hydrocarbon

generation potential. The OM types are II<sub>1</sub> and III. The Late Paleozoic samples are highly mature source rocks.

The original OM abundance was determined by applying a weathering correction and calculating the original OM abundance using analogy and chemical kinetic methods, respectively. The samples from these three formations meet the standard of effective source rocks, and several samples from the Linxi Formation meet the effective source rock standard. The original hydrocarbon generation potential of mudstone from the Linxi Formation is higher than those of mudstones from the Benbatu Formation and Zhesi Formation.

The OM sources can reflect the original capacity of these source rocks to generate hydrocarbons. The primary sources of the source rock samples in this study

are low-level aquatic organisms, which can form high-quality kerogen with a favourable original hydrocarbon generation capacity. Comparisons between original and residual hydrocarbon generation potentials reveal that hydrocarbons have been generated and discharged.

The methods used in this study to determine the original hydrocarbon generation potential and original TOC content to evaluate source rocks can potentially be used as a reference for future investigations of highly maturity Paleozoic source rocks in poorly explored areas.

#### ACKNOWLEDGMENTS

The authors gratefully acknowledge all editors for working on this article. The authors gratefully acknowledge associated editor (Dr Yu.I. Galushkin) for working on this article. The authors gratefully acknowledge all reviewers for reviewing this article.

#### FUNDING

This study was funded by the National Natural Science Foundation of China (project no. 41430322).

#### CONFLICT OF INTEREST

The authors declare that they have no conflicts of interest.

#### REFERENCES

- R. Bertrand, "Correlations among the reflectances of vitrinite, chitinozoans, graptolites and scolecodonts," *Org. Geochem.* **15**, 565–574 (1990).
- G. Chen, S. Lu, J. Zhang, Q. Xue, T. Han, H. Xue, S. Tian, J. Li, C. Xu, and P. Marina, "Keys to linking GCMC simulations and shale gas adsorption experiments," *Fuel* **199**, 14–21 (2017a).
- L. Chen, Z. Jiang, K. Liu, J. Tan, F. Gao and P. Wang, "Pore structure characterization for organic-rich Lower Silurian shale in the Upper Yangtze Platform, South China: A possible mechanism for pore development," *J. Nat. Gas. Sci. Eng.* **46**, 1–15 (2017b).
- J. L. Clayton, "Subaerial weathering of sedimentary organic matter," *Geochim. Cosmochim. Ac.* **42**, 305–312 (1978).
- S. M. Colman, "Rock-weathering rates as functions of time," *Quat. Res.* **15**, 250–264 (1981).
- G. P. Cooles, A. S. Mackenzie and T. M. Quigley, "Calculation of petroleum masses generated and expelled from source rocks," *Org. Geochem.* **10**, 235–245 (1986).
- B. M. Didyk, B. R. T. Simoneit, S. C. Brassell and G. Eglington, "Organic geochemical indicators of palaeoenvironmental conditions of sedimentation," *Nature* **272**, 216–222 (1978).
- E. Esemé, R. Littke, B. M. Krooss and J. Schwarzbauer, "Experimental investigation of the compositional variation of petroleum during primary migration," *Org. Geochem.* **38**, 1373–1397 (2007).
- J. Espitalie, G. Deroo and F. Marquis, "La pyrolyse Rock-Eval et ses applications. Première partie," *Rev. Inst. Fr. Pét.* **40**, 563–579 (1985).
- M. G. Fowler and L. D. Stasiuk, "Devonian hydrocarbon source rocks and their derived oils in the Western Canada Sedimentary Basin," *B. Can. Petrol. Geol.* **49**, 117–148 (2001).
- C. Han, F. Jin, J. Wang, Z. Gao, J. Wu and Q. Cui, "Exploration prospect of hydrocarbon of Neopaleozoic in Erlian basin, Inner Mongolia, China," *Geol. Bull. China* **30**, 243–249 (2011) [in Chinese with English abstract]. <https://doi.org/10.3969/j.issn.1671-2552.2011.02>
- A. Hatampour, "Using rock eval pyrolysis for studying the hydrocarbon potential of the Pabdeh Formation in Ziluee Oilfield, south west of Iran," *Petrol. Sci. Technol.* **32**, 1586–1597 (2014).
- D. Hou, *Petroleum Geochemistry* (Petroleum industry press, Beijing, 2011) [in Chinese].
- X. Li, "The influence of weathering on organic matter in surface samples," *Pet. Explor. Dev.* **5**, 24–31 (1985) [in Chinese with English abstract].
- D. Liu, W. Zhang, Q. Kong, Z. Feng, C. Fang and W. Peng, "Lower Paleozoic source rocks and natural gas origins in Ordos Basin, NW China," *Pet. Explor. Dev.* **43**, 591–601 (2016). [https://doi.org/10.1016/S1876-3804\(16\)30069-6](https://doi.org/10.1016/S1876-3804(16)30069-6)
- Y. Liu, X. Zhang, X. Chi, Q. Wen, C. Liang, G. Han, L. Zhao and Y. Zhao, "Deformation and tectonic layer division of the Upper Paleozoic in Daxing'anling area," *J. Jilin Univ., Earth Sci. Ed.* **41**, 1304–1313 (2011) [in Chinese with English abstract]. <https://doi.org/10.3969/j.issn.1000-3657.2010.04.010>.
- S. Lu, H. Xue and N. Zhong, "Simulating calculation of the variations of organic matter abundance and hydrocarbon-generating potential during geological processes," *Geol. Rev. (Beijing, China)* **49**, 292–297 (2003) [in Chinese]. <https://doi.org/10.3321/j.issn:0371-5736.2003.03.011>
- L. Marynowski, S. Kurkiewicz, M. Rakocinski and B. R. T. Simoneit, "Effects of weathering on organic matter: I. Changes in molecular composition of extractable organic compounds caused by paleoweathering of a Lower Carboniferous (Tournaisian) marine black shale," *Chem. Geol.* **285**, 144–156 (2011).
- A. S. Pepper, "Estimating the petroleum expulsion behaviour of source rocks: a novel quantitative approach," *Geol. Soc. London, Spec. Publ.* **59**, 9–31 (1991).
- S. Rao, C. Zhu, Q. Wang, X. Tang, W. Li, G. Jiang, S. Hu and J. Wang, "Thermal evolution patterns of the Sini-an–Lower Paleozoic source rocks in the Sichuan basin, southwest China," *Chin. J. Geophys.* **56**, 1549–1559 (2013) [in Chinese]. <https://doi.org/10.6038/cjg20130513>
- M. H. Saberi, A. R. Rabbani and M. Ghavidel-syooki, "Hydrocarbon potential and palynological study of the Latest Ordovician–Earliest Silurian source rock (Sarchahan Formation) in the Zagros Mountains, southern Iran," *Mar. Petrol. Geol.* **71**, 12–25 (2016).
- R. S. Scalan and J. E. Smith, "An improved measure of the odd-even predominance in the normal alkanes of sediment extracts and petroleum," *Geochim. Cosmochim. Acta.* **34**, 611–620 (1970).

- A. Schito, S. Corrado, M. Trolese, L. Aldega, C. Caricchi, S. Cirilli, D. Grigo, A. Guedes, C. Romano, A. Spina and B. Valentim, "Assessment of thermal evolution of Paleozoic successions of the Holy Cross Mountains (Poland)," *Mar. Petrol. Geol.* **80**, 112–132 (2017).
- P. Sobolev, D. Franke, C. Gaedicke, J. Kus, G. Scheeder, K. Piepjohn, C. Brandes, M. Blumenberg and B. Mouly, "Reconnaissance study of organic geochemistry and petrology of Paleozoic–Cenozoic potential hydrocarbon source rocks from the New Siberian Islands, Arctic Russia," *Mar. Petrol. Geol.* **78**, 30–47 (2016).
- M. Teichmuller and M. Wolf, "Application of fluorescence microscopy in coal petrology and oil exploration," *J. Microsc.* **1**, 49–73 (1977).
- B. P. Tissot and D. H. Welte, *Petroleum Formation and Occurrence* (Springer-Verlag, 1984).
- M. Vandenbroucke and C. Largeau, "Kerogen origin, evolution and structure," *Org. Geochem.* **38**, 719–833 (2007).
- C. Wang, W. Jin, X. Zhang, Z. Ma, X. Chi, Y. Liu and N. Li, "New understanding of the Late Paleozoic tectonics in Northeastern China and adjacent areas," *J. Stratigraphy* **32**, 119–136 (2008) [in Chinese].  
<https://doi.org/10.3969/j.issn.0253-4959.2008.02.001>
- J. Wei, C. Lu, X. Wei, W. Han and T. Jiang, "The influence of intense weathering on the evaluation indexes of hydrocarbon source rocks: A case study of Carboniferous–Permian Strata of Ejin Banner and its neighboring areas," *Geol. Bull. China* **31**, 1715–1723 (2012) [in Chinese with English abstract].  
<https://doi.org/10.3969/j.issn.1671-2552.2012.10.016>
- Y. Yang, Y. Ma, C. Liu, H. Cheng and Z. Li, "Influence of weathering on abundance of source rocks: A case study of Keluke Formation of Upper Carboniferous in the Shihuigou area, North Margin of Qaidam Basin," *Earth Sci. Front.* **23**, 113–118 (2016) [in Chinese].  
<https://doi.org/10.13745/j.esf.2016.05.012>
- D. Zhai, Y. Zhang, S. Tian, F. Wu, E. Xing, M. Wang, L. Shi and Z. Wang, "Sedimentary environment and evolution of the Upper Permian Linxi Formation in Linxi area, Inner Mongolia," *J. Palaeogeogr.* **17**, 359–370 (2015) [in Chinese].  
<https://doi.org/10.7605/gdtxb.2015.03.030>
- J. Zhang, D. Wang, J. Qin and B. Liu, "Study on the weathering correction of source outcrop samples from the Qinghai–Tibet plateau," *Pet. Geol. Exp.* **23**, 297–300 (2001) [in Chinese].  
<https://doi.org/10.3969/j.issn.1001-6112.2001.03.009>
- T. Zhang, G. S. Ellis, S. C. Ruppel, K. Milliken and R. Yang, "Effect of organic-matter type and thermal maturity on methane adsorption in shale-gas systems," *Org. Geochem.* **47**, 120–131 (2012).
- X. Zhang, J. Zhou, X. Chi, C. Wang and D. Hu, "Late Paleozoic tectonic-sedimentation and petroleum resources in Northeastern China," *J. Jilin Univ., Earth Sci. Ed.* **38**, 719–725 (2008) [in Chinese].  
<https://doi.org/10.3969/j.issn.1671-5888.2008.05.001>
- M. Zhao, Z. Wang, W. Pan, S. Liu, S. Qin and J. Han, "Lower Palaeozoic source rocks in Manjiaer Sag, Tarim Basin," *Pet. Explor. Dev.* **35**, 417–423 (2008) [in Chinese].  
<https://doi.org/10.3321/j.issn:1000-0747.2008.04.004>

**Publisher's Note.** Pleiades Publishing remains neutral with regard to jurisdictional claims in published maps and institutional affiliations.